THE JOURNAL OF BIOLOGICAL CHEMISTRY VOL. 288, NO. 2, pp. 1307–1316, January 11, 2013

An Inhibitory Antibody against Dipeptidyl Peptidase IV Improves Glucose Tolerance *in Vivo*

Received for publication, June 29, 2012, and in revised form, November 9, 2012 Published, JBC Papers in Press, November 26, 2012, DOI 10.1074/jbc.M112.396317

Jie Tang[‡1], Jiangwen Majeti[§], Athena Sudom[¶], Yumei Xiong[§], Mei Lu[‡], Qiang Liu[‡], Jared Higbee[‡], Yi Zhang[‡], Yan Wang[‡], Wei Wang[‡], Ping Cao[‡], Zhen Xia[‡], Sheree Johnstone[¶], Xiaoshan Min[¶], Xiaoping Yang[‡], Hui Shao[‡], Timothy Yu[‡], Nik Sharkov[‡], Nigel Walker[¶], Hua Tu[§], Wenyan Shen[‡], and Zhulun Wang[¶2]

From the Departments of [‡]Biologics, [§]Metabolic Disorders, and [¶]Molecular Structure, Amgen Inc., South San Francisco, California 94080

Background: Suppression of DPP-IV activity improves type 2 diabetic symptoms.
Results: Inhibitory antibodies suppress DPP-IV activity, promote glucose tolerance, and increase plasma GLP-1 levels in hyperglycemic Zucker fatty rats.
Conclusion: Inhibitory antibody against DPP-IV offers pro-incretin effects *in vivo*.
Significance: This study validates a large molecule approach for targeting DPP-IV activity.

Dipeptidyl peptidase IV (DPP-IV) degrades the incretin hormone glucagon-like peptide 1 (GLP-1). Small molecule DPP-IV inhibitors have been used as treatments for type 2 diabetes to improve glucose tolerance. However, each of the marketed small molecule drugs has its own limitation in terms of efficacy and side effects. To search for an alternative strategy of inhibiting DPP-IV activity, we generated a panel of tight binding inhibitory mouse monoclonal antibodies (mAbs) against rat DPP-IV. When tested *in vitro*, these mAbs partially inhibited the GLP-1 cleavage activity of purified enzyme and rat plasma. To understand the partial inhibition, we solved the co-crystal structure of one of the mAb Fabs (Ab1) in complex with rat DPP-IV. Although Ab1 does not bind at the active site, it partially blocks the side opening, which prevents the large substrates such as GLP-1 from accessing the active site, but not small molecules such as sitagliptin. When Ab1 was tested *in vivo*, it reduced plasma glucose and increased plasma GLP-1 concentration during an oral glucose tolerance test in rats. Together, we demonstrated the feasibility of using mAbs to inhibit DPP-IV activity and to improve glucose tolerance in a diabetic rat model.

Serine protease dipeptidyl peptidase IV (DPP-IV)[3] (also referred to as CD26) is a type II membrane protein that modulates biological activities of peptide hormones, cytokines, and neuropeptides by removing two residues from the N termini of these peptides (1–3). DPP-IV is well conserved across species. Human DPP-IV shares 85% sequence identity with rat DPP-IV (3, 4). Membrane-bound DPP-IV functions as a peptidase as well as binding partner for other proteins, such as adenosine deaminase and T-cell antigen (CD45), and is involved in T-cell co-stimulation and tumor suppression (4, 5). DPP-IV also exists in soluble form (residues 39–766) in plasma as a result of proteolysis near the N-terminal transmembrane domain (6). Soluble and membrane-bound forms of DPP-IV have similar catalytic activities. *In vivo*, DPP-IV proteins are heavily glycosylated and exist as homodimers, where each subunit is comprised of two structural domains: the α/β-hydrolase and β-propeller domains (4). The catalytic site is located in a large cavity formed between these two domains. There are two structural holes in DPP-IV that could serve as substrate access and product discharge routes for catalysis: a tunnel through the β-propeller domain (propeller opening) and a side opening formed between the interface of the β-propeller domain and catalytic domain (7–10).

Suppression of DPP-IV activity is an established strategy to treat type 2 diabetes mellitus, which is a chronic disease characterized by elevated blood glucose levels and attenuated response to insulin (11–14). DPP-IV inactivates incretins, especially GLP-1 and GIP, which are released from the gut during meals and serve as enhancers of glucose-dependent insulin release from pancreatic β-cells (15). Because of DPP-IV activity and the small sizes of GLP-1 and GIP, their half-lives are less than 1 min. Several therapeutic strategies, including administration of exogenous GLP-1 or DPP-IV-resistant GLP-1 analogues and inhibition of DPP-IV with small molecule inhibitors, have been explored as potential treatments for type 2 diabetes (12, 16–19). To date, a few GLP-1 analogues and a number of small molecule DPP-IV inhibitors have either become marketed products or are at different stages of clinical development. Currently, five small molecule DPP-IV inhibitors have been approved as antihyperglycemic drugs for type 2 diabetes. They are linagliptin, sitagliptin, vildagliptin, saxagliptin, and alogliptin (13, 20, 21). In humans, the approved compounds are generally well tolerated and demonstrate various degrees of efficacy in treating type 2 diabetes at recommended doses, sug-

[S] This article contains supplemental Table S1 and Figs. S1 and S2.
The atomic coordinates and structure factors (codes 4FFV and 4FFW) have been deposited in the Protein Data Bank (http://wwpdb.org/).

[1] To whom correspondence may be addressed: Dept. of Biologics, Amgen Inc., 1120 Veterans Blvd., South San Francisco, CA 94080. Tel.: 650-244-2542; E-mail: jiet@amgen.com.
[2] To whom correspondence may be addressed: Dept. of Molecular Structure, Amgen Inc., 1120 Veterans Blvd., South San Francisco, CA 94080. Tel.: 650-244-2446; E-mail: zwang@amgen.com.

[3] The abbreviations used are: DPP-IV, dipeptidyl peptidase IV; GLP-1, glucagon-like peptide 1; GIP, glucose-dependent insulinotropic polypeptide; 6-FAM, 6-carboxyfluorescein; HBS, HEPES-buffered saline; CDR, complementarity-determining regions; SDF, stromal cell-derived factor; Ab, antibody; GP-pNA, H-Gly-Pro-p-nitroanilide.

gesting that inhibition of DPP-IV activity represents a desirable therapeutic approach for type 2 diabetes (13, 22–25). However, adverse effects such as nausea, common cold-like symptoms, and pancreatitis have been reported for approved DPP-IV inhibitors (25). Most of the small molecules are competitive reversible inhibitors with different degrees of selectivity toward other family members of prolyl peptidases such as DPP-VIII and DPP-IX. These inhibitors have been implicated in preclinical toxicities, including suppression of T-cell activation and proliferation in some studies (26).

Antibodies have been widely used as therapeutic agents for a variety of diseases (27, 28). In general, they function to modulate receptor activity, neutralize soluble ligands, and deliver cytotoxic compounds to target tissues. Antibodies have excellent attributes as pharmacologic agents because of their high specificities and long *in vivo* half-lives. Proteases generally have a cavity in the catalytic site that accommodates substrates and cleaves the substrate peptide bonds. Previously, highly selective inhibitory antibodies have been identified for proteases with one structural opening for substrates (29–31). These antibodies interact directly with loops near the substrate-binding site, thus blocking substrates from accessing the active site. Here we describe identification of an inhibitory antibody against DPP-IV that improves glucose tolerance and plasma GLP-1 concentrations in a rat diabetic model. Through this antibody, we demonstrated that an inhibitory antibody for DPP-IV could be used to raise plasma GLP-1 concentration and improve glucose tolerance in a rat diabetic model. Our results support the hypothesis of using a DPP-IV inhibitory antibody as a therapy for type 2 diabetes.

EXPERIMENTAL PROCEDURES

Rat DPP-IV and DPP-IV Activity Assays—cDNA of rat DPP-IV (residues 37–767) was fused at the 3′ end to a sequence encoding a C-terminal His_8 tag and at the 5′ end to a sequence coding for an IgGκ light chain signal peptide. This rat DPP-IV construct was transiently expressed in 293 6E cells. Conditioned media, which contained secreted soluble DPP-IV, were harvested, and DPP-IV proteins were purified using affinity chromatography followed by size exclusion chromatography. In the affinity chromatography step, conditioned media were concentrated and buffer-exchanged against 20 mM Tris-HCl, pH 7.9, 1 M NaCl, and 20 mM imidazole. Rat DPP-IV was captured on a nickel-immobilized metal ion affinity chromatography column, and nonspecific interactions were removed by washing with the binding buffer. Rat DPP-IV was recovered by eluting with 250 mM imidazole in 20 mM Tris-HCl, pH 7.3, 0.5 M NaCl. The recovered rat DPP-IV was polished on a Superdex 200 exclusion chromatography column and formulated in 25 mM HEPES, pH 7.6, 150 mM NaCl.

The dipeptidyl peptidase activity of DPP-IV was measured by monitoring cleavage of a peptide substrate GP-pNA. In the reaction, DPP-IV was used to cleave 1 mM substrate in PBS. Cleavage of GP-pNA was monitored by $\Delta A_{405\ nm}$.

GLP-1 Degradation and DPP-IV Inhibition Assays—Proteolytic cleavage of GLP-1 (residues 7–36) to GLP-1 (residues 9–36) by recombinant DPP-IV was monitored using alpha screening and HPLC assays. In the alpha screening assay, C-terminal biotinylated GLP-1 (residues 7–36) was cleaved by recombinant DPP-IV. At specific time points, an aliquot of reaction mix was quenched by adding sitagliptin to a final concentration of 1 μM, and the amount of intact C-terminal biotinylated GLP-1 (residues 7–36) was quantitated by alpha screening with a streptavidin-coated donor bead and GLP-1 (residues 7–36) specific antibody-coated acceptor beads. In the HPLC assay, 12 μM GLP-1 C-terminal amide was cleaved by 1.78 nM recombinant rat DPP-IV in PBS containing 0.1% BSA. At each time point, 40 μl of reaction mix was withdrawn, and the reaction was stopped by adding 60 μl of 8 M guanidine-HCl, 0.5% TCA. Substrate, GLP-1 (residues 7–36), and product, GLP-1 (residues 9–36), were resolved on a Jupiter C18 column (2.1 × 150 mm) with an acetonitrile gradient of 32–45% that contained 0.1% TFA in 6 min at a flow rate of 0.3 ml/min. Integration of chromatogram $A_{280\ nm}$ peak area was used to quantitate the amount of GLP-1.

Inhibition of DPP-IV by monoclonal DPP-IV antibodies was analyzed by measuring the GLP-1-cleaving activity of rat DPP-IV proteins in the presence of increasing amounts of mAbs. In Fig. 1*A*, rat DPP-IV was incubated for 60 min with mAbs against rat DPP-IV or control mAb. The reaction was started by adding GLP-1 (residues 7–36) and reaction buffer to bring the final concentrations of GLP-1 and rat DPP-IV to 12 μM and 1.78 nM, respectively, in a 40-μl reaction volume. Twenty-three minutes after adding GLP-1, the reactions were stopped by adding 60 μl of 8 M guanidine-HCl in 0.5% trichloroacetic acid (TCA) to bring the volume to 100 μl. Reaction samples were analyzed on C18 reverse phase-HPLC, and concentrations of GLP-1 (residues 7–36) and GLP-1 (residues 9–36) were estimated from integrated $A_{280\ nm}$ peak areas of GLP-1 peaks. V_i is calculated as product (GLP-1 (residues 9–36)) accumulation rate (nM/min) in the presence of mAb. V_0 is product accumulation rate (nM/min) in the absence of any mAb. V_i/V_0% represents the degree of inhibition of DPP-IV by mAbs. In Fig. 1*B*, rat DPP-IV was incubating with varying amounts of Ab1, Ab2, and Ab3 for 60 min. Reactions were set up similarly as in *panel A*. At time points of 0, 10, 20, 30, 40, 50, and 60 min after the addition of GLP-1, 20 μl of reaction mix was withdrawn, and the reaction was stopped by adding 30 μl of 8 M guanidine-HCl in 0.5% TCA. Concentrations of GLP-1 (residues 7–36) and GLP-1 (residues 9–36), and degree of inhibition (V_i/V_0%) were estimated as in *panel A*. IC_{50} was estimated by nonlinear fitting of the percentage of inhibition to mAb concentration using GraphPad Prism software. Cleavage of GIP (Sigma G2269) by rat DPP-IV was analyzed similarly as for GLP-1 except that GIP was cleaved at 4 μM (supplemental Fig. S2).

Cleavage of GLP-1 by rat plasma containing DPP-IV was analyzed by monitoring the proteolysis of a fluorescent GLP-1 conjugate (GLP-1 (residues 7–36)-Lys(6-FAM) amide; Bachem 2000343) using HPLC. To analyze mAb inhibition of GLP-1 cleavage in rat plasma, 4.5 μl of 1 M Tris-HCl, pH 7.5, was used to adjust the pH of rat plasma (72.5 μl). Increasing amounts of DPP-IV mAbs or control mAb were incubated with the buffered rat plasma for 60 min at room temperature. DPP-IV activity in the treated plasma samples was assessed by monitoring the proteolysis of the FAM-labeled GLP-1 substrate in a 90-μl

cleavage reaction. Progression of the catalytic reaction was monitored by withdrawing 30 μl of reaction mix and stopping the reaction with 30 μl of 8 M guanidine-HCl in 0.5% TCA at time points of 30, 60, and 90 min. For the 0-min time point, 30 μl of reaction mix was added with 8 M guanidine-HCl in 0.5% TCA and GLP-1 (FAM) at the same time. Substrate GLP-1 (residues 7–36) and product GLP-1 (residues 9–36) were quantitated by HPLC analysis that monitored FAM fluorescence (excitation = 495 nm, emission = 517 nm) on a Jupiter C4 column. Degree of inhibition (V_i/V_0%) and IC_{50} were calculated similarly as in Fig. *1B*.

Antibody Generation and Characterization—Monoclonal antibodies against rat DPP-IV were generated by immunizing C57BL/6 mice with purified soluble rat DPP-IV transiently expressed in 293 6E cells. B-cells from immunized mice were harvested and fused to a nonsecretory mouse myeloma cell line Sp2/0-Ag14 (ATCC, Manassas, VA) to generate hybridomas using standard techniques. Conditioned media from hybridoma clones were first screened for rat DPP-IV binding activity by ELISA using biotinylated rat DPP-IV as the capture antigen followed by characterization of DPP-IV inhibitory activity using the alpha screening method. Positive clones that showed inhibitory activity against DPP-IV in alpha screening were further characterized using the HPLC-based inhibition assays described above.

Competition ELISA was used to group the inhibitory mAb clones. Monoclonal antibodies against rat DPP-IV were coated on the ELISA plate surface and used to capture biotinylated rat DPP-IV. Captured DPP-IV was detected with HRP-labeled streptavidin. To group the positive mAbs, mAb-coated ELISA plates were used to capture biotinylated rat DPP-IV that was preincubated with other individual mAbs. When two mAbs are in the same epitope bin, the signal of DPP-IV in the competition ELISA is decreased.

Monoclonal antibodies were expressed and purified as described previously (32). Briefly, mAbs were expressed in 293 6E cells or in hybridoma clones. Expressed mAbs were secreted into conditioned media and captured on MabSelect SuRe columns, which had been equilibrated with Tris- or HEPES-buffered saline solutions (TBS or HBS). After washing with TBS or HBS, bound IgG proteins were eluted with 0.5% acetic acid, pH 3.5. Eluted IgG molecules were further polished on SP-Sepharose or Superdex 200 to remove aggregates. The Ab1 Fab fragment was prepared by digesting full antibody molecules with immobilized papain (Thermo Scientific) according to the manufacturer's instructions. The Fab molecules were recovered by passing through a MabSelect SuRe column for Fc fragment removal and were formulated in 10 mM acetate buffer solution, pH 5.2, 150 mM NaCl using dialysis.

Binding Affinity—Binding of mAb to rat DPP-IV proteins was measured using the KinExa 3000 (Sapidyne Instruments) and ForteBio protein G chip on Octet96 according to manufacturer's recommendations and as described previously for analyzing mAb-antigen interactions (32). In Octet96 analysis, Ab1 at 300 μg/ml first bound to the protein G tip in HBS. Then Ab1 on the protein G tip was used to bind to rat DPP-IV or control proteins in HBS or in 293 cell lysate (2 mg/ml in HBS) (supplemental Fig. S1).

X-ray Crystallography—The purified DPP-IV·Ab1 Fab complex was concentrated to 7 mg/ml in 20 mM Tris, pH 7.9, 200 mM NaCl. Crystals were grown at 20 °C in sitting drops with 1.5 μl of protein solution plus 1.5 μl of reservoir solution of 2.2–2.7 M ammonium sulfate in Tris buffer, pH 7.5–9.0. To obtain the ternary complex of DPP-IV·Ab1·a small molecule inhibitor (sitagliptin), purified DPP-IV·Fab complex at 7 mg/ml was incubated with sitagliptin at 0.3 mM for 2–3 h before crystallization. For x-ray diffraction data collection, crystals were transferred into well solution with 20% (w/v) of ethylene glycol and flash-frozen in liquid nitrogen.

The x-ray diffraction data were collected at the synchrotron beamline 502 at Advanced Light Source (ALS) (Berkeley, CA) and processed with program MOSFLM (33) and SCALA (34) in the CCP4 program suite (35). The structure was solved to a resolution of 2.5 Å by molecular replacement method MOLREP (36) using a previously published human DPP-IV structure (Protein Data Bank (PDB) code: 2OGZ) (37)) as a search model for DPP-IV, and a Fab structure (PDB code: 1A6T) (38) as a search model for Ab1. Model building and refinement were carried out in COOT (39) and REFMAC (40) in CCP4, respectively (supplemental Table S1). All structural figures were prepared using PyMOL (46).

Studies in Rat Models—Zucker fatty rats were fed with 11% breeder chow. In an oral glucose tolerance test, 4-h-fasted male Zucker fatty rats (13–14 week, Harlan Laboratories) were intravenously dosed with anti-DPP-IV (20 mg/kg) or IgG control (20 mg/kg) at −90 min followed by oral gavage of sitagliptin (30 mg/kg) at −40 min. We used a high dose of Ab1 and sitagliptin to promote complex formation of DPP-IV·Ab1 and DPP-IV·sitagliptin in our initial animal efficacy study. At time 0, animals were orally administered with 2 g/kg glucose. Blood glucose levels were measured at −90, 0, 10, 30, 60, 90, and 120 min by glucose strip. Blood samples were collected at −90, 0, 10, 30, and 60 min, and GLP-1 and insulin concentrations were measured using a GLP-1 quantitation kit from Linco and a rat insulin quantitation kit from Alpco.

RESULTS

Generation of Inhibitory Antibodies against Rat DPP-IV—C57BL/6 mice were immunized with dimeric rat DPP-IV. B-cells from immunized mice were fused to nonsecretory myeloma cells to generate hybridomas. Approximately 2900 antibody clones that bind rat DPP-IV were identified by ELISA screening with purified rat DPP-IV protein as the capturing agent. From these clones, 13 were selected based on their inhibitory activity in the GLP-1 degradation alpha screening assay. These 13 antibodies were grouped into three noncompeting bins based on competition ELISA assay.

Identification of Specific High-affinity Partial Inhibitory Antibodies—Affinities of mAbs representing each of the three epitope bins (Ab1, Ab2, and Ab3) were analyzed in a KinExa-based solution equilibrium binding assay using purified rat DPP-IV dimers as antigens. The affinities for rat DPP-IV are ~10, 7.5, and 117 pM for Ab1, Ab2, and Ab3, respectively (Table 1). Although Ab1 binds to rat DPP-IV with high affinity, it shows minimum binding for human DPP-IV and DPP-IX,

TABLE 1
Binding affinities of mouse mAbs to rat DPP-IV

Sample ID for mAb	Against rat DPP-IV	
	K_d[a]	95% confidence interval
	pM	pM
Ab1	10	4–22
Ab2	7.5	1–23
Ab3	117	100–125

[a] K_d is obtained from nonlinear regression of the competition curves using KinExA Pro software.

bovine serum albumin, and proteins in 293 cell lysate (supplemental Fig. S1).

All 13 mAbs from the three bins were tested for inhibitory activity toward rat DPP-IV. When small chromogenic peptides (GP-pNA) were used as substrates, none of the 13 antibodies inhibited DPP-IV activity (supplemental Fig. S2).[4] To confirm and assess the inhibitory activities observed in the alpha screening assay, we performed a more quantitative HPLC assay using GLP-1 as a substrate (Fig. 1*A*). Nonbinding control mAb or noninhibitory rat DPP-IV binder clone (Ab10) showed no inhibitory activity against DPP-IV-mediated cleavage of GLP-1 (Fig. 1*A*). In contrast, all putative inhibitory mAbs demonstrated inhibition of DPP-IV activity by 60–80% at saturating antibody concentrations, suggesting that these mAbs are partial inhibitors. The top three candidates, *i.e.* Ab1, Ab2, and Ab3, displayed IC_{50} values of 0.79, 0.6, and 1.02 nM, respectively (Fig. 1*B*). These values approach half of the DPP-IV concentration used in the assay, indicating the tight affinity nature of the bindings. The tight binding affinities of these inhibitory mAbs agreed with the K_d results obtained from affinity measurement.

To further confirm the ability of the mAb to inhibit DPP-IV activity under more physiological conditions, we analyzed the effects of Ab1 and Ab2 on GLP-1-cleaving activity in rat plasma (Fig. 2). Results from this experiment indicated that Ab1 and Ab2 inhibited the conversion of FAM-labeled GLP-1 (residues 7–36) (substrate) to GLP-1 (residues 9–36) (product) at IC_{50} of 6.8 and 5.9 nM, respectively. Likewise, the two antibodies only partially inhibited the GLP-1-degrading activity of the plasma by 45% at the condition used. The data confirm the partial inhibitory activity of Ab1 and Ab2 for endogenous DPP-IV in rat plasma.

Structural Elucidation of Partial Inhibition by Ab1—To elucidate the molecular mechanism of partial inhibition of these mAbs, we solved the x-ray co-crystal structure of DPP-IV in complex with Ab1 Fab. The binary complex structure was determined to a resolution of 2.4 Å in a space group of $P2_1$ with two copies of the complex in an asymmetrical unit. Overall, the structure is well ordered except for the constant domains of Fab, which are highly flexible.

The structure of DPP-IV·Ab1 Fab complex reveals a homodimer of DPP-IV proteins with each monomer binding one Fab molecule (Fig. 3*A*). The DPP-IV dimer is nearly identical to the previously reported apo structure of rat DPP-IV (PDB code: 2GBC) (41) with a root mean square deviation of 0.47 Å for 1300 Cα atoms from the dimer. Each DPP-IV monomer adopts a two-domain architecture of N-terminal eight-blade β-propeller and C-terminal catalytic α/β-hydrolase fold. The active site is located in the large central cavity, which contains two openings to the outside. The propeller opening, located in the center of the β-propeller domain, has a pore size of about 9 × 16 Å (Fig. 3*B*). The side opening between the N- and C-terminal domains is rather large with a dimension of about 16 × 22 Å (Fig. 3*B*). The distances from the active site to the protein surface are ~20 and 35 Å through the side opening and the propeller opening, respectively. Due to the size difference of these two openings, it is suggested that the side opening serves as the entrance path for the substrates and the propeller/side opening serves as the exit route (7–10).

Ab1 Fab binds to the side of the β-propeller domain of DPP-IV. The recognition of Ab1 is mediated mainly by three CDR loops in the heavy chain and CDR loop 3 in the light chain (Fig. 3*C*). The key epitope on DPP-IV is located in the linker region between blade 1 and blade 2 of the β-propeller, with amino acid sequence of ^{89}ENSTFEIFGD^{98}, in which Glu-94 and Ile-95 make close van der Waals interactions with the Fab of Ab1 (Fig. 3*D*). Interestingly, the corresponding sequence for human DPP-IV in this region is ^{91}ENSTFDEFGH^{100} (supplemental Fig. S1*B*). The mutation of the critical epitope residues Glu-94 and Ile-95 in rat DPP-IV to Asp-96 and Glu-97 in human protein rationalizes the lack of cross-reactivity of Ab1 to human DPP-IV and the high specificity of Ab1.

As the heavy chain of the CDR region of Ab1 plays a major role in epitope recognition to DPP-IV, the light chain CDR loops are situated at the side opening. Due to the large size of this side aperture, however, Ab1 Fab does not block this opening completely, leaving enough space for smaller substances but not large substrates to access the catalytic site (Fig. 3*E*). To confirm this structural observation, we co-crystallized the substrate peptide GLP-1 or a small molecule inhibitor sitagliptin with DPP-IV·Fab complex. Although the co-crystal structure of DPP-IV·Ab1 in the presence of GLP-1 shows an unoccupied active site, the ternary co-crystal structure including sitagliptin shows the inhibitor bound at the active site (Fig. 4*A*). The complex structure of DPP-IV·Fab·sitagliptin reveals very little change in the binding mode of sitagliptin in comparison with the previously reported co-crystal structure of sitagliptin with human DPP-IV (PDB code: 1X70) (42) as well as the active site and Ab1 binding (Fig. 4*B*). Thus, Ab1 does not blockade the DPP-IV substrate-binding site directly; instead it restricts the substrate path to the catalytic site. The structural data provide a sensible molecular basis for the observed partial inhibitory activity for these mAbs.

In Vivo Efficacy of Ab1—To investigate whether Ab1 could improve glucose tolerance and raise GLP-1 concentration *in vivo*, we tested Ab1 in a Zucker fatty rat diabetic model using sitagliptin as a positive control (Fig. 5). In this experiment, we observed that in oral glucose tolerance test analyses, Ab1 improved glucose tolerance and had similar efficacy in improving glucose tolerance as sitagliptin control (Fig. 5*A*). At time points of 60 and 90 min after glucose challenge, Ab1 reduced glucose level from an average of 299.4 mg/dl to an average of 228.9 mg/dl with $p < 0.0001$ (60-min time point) and from an average of 287.6 mg/dl to an average of 229.8 mg/dl with $p <$

[4] J. Tang, unpublished data.

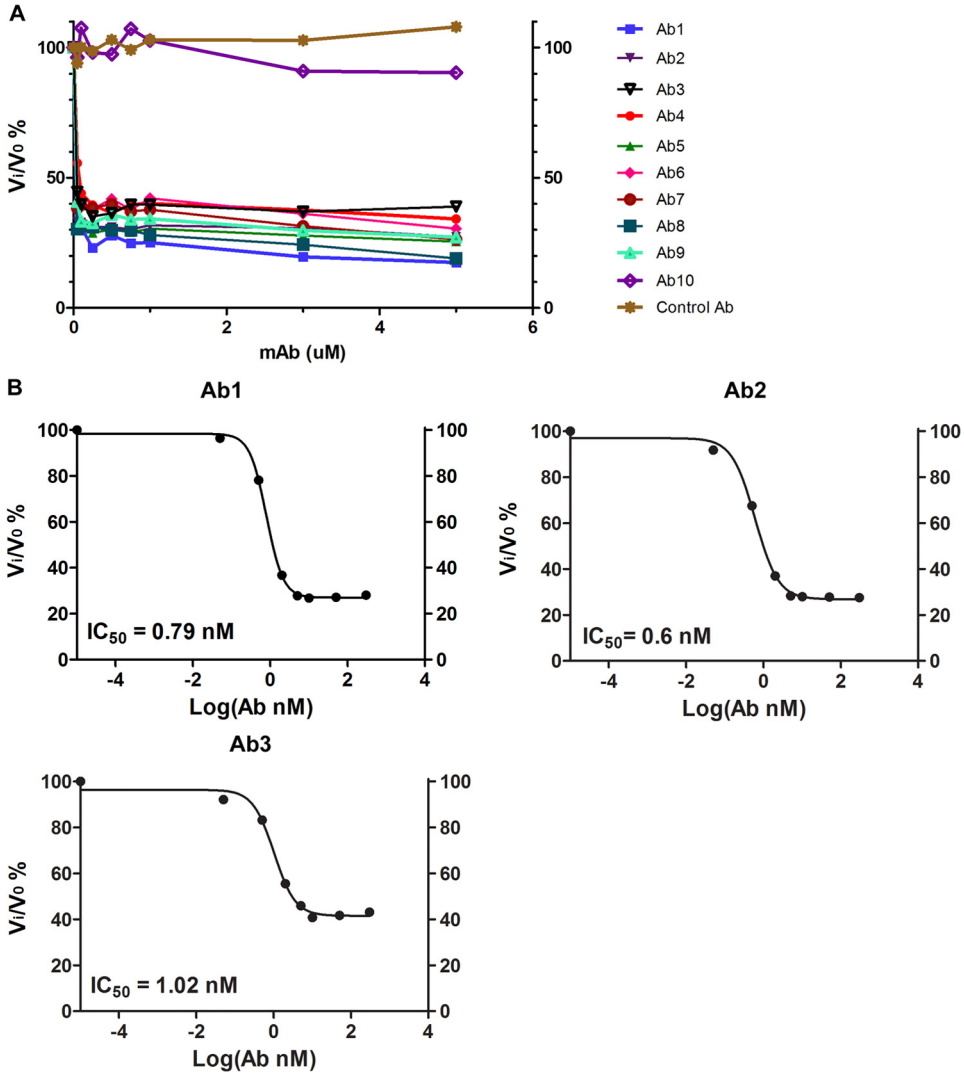

FIGURE 1. **Identification of inhibitory antibodies for rat DPP-IV.** *A*, inhibition of rat DPP-IV by mAbs against rat DPP-IV: inhibition profiles at varying concentrations of a subset of nine good expressers (Ab1–9) from the 13 identified in the alpha screening assay plus two control mAbs (control antibody for irrelevant nonbinding mAb and Ab10 for binding, noninhibitory antibody). *B*, mAb IC_{50} values for Ab1, Ab2, and Ab3 toward recombinant rat DPP-IV enzyme: inhibition of DPP-IV-mediated cleavage of GLP-1 by inhibitory antibodies. IC_{50} was estimated by nonlinear fitting of the percentage of inhibition to mAb concentration.

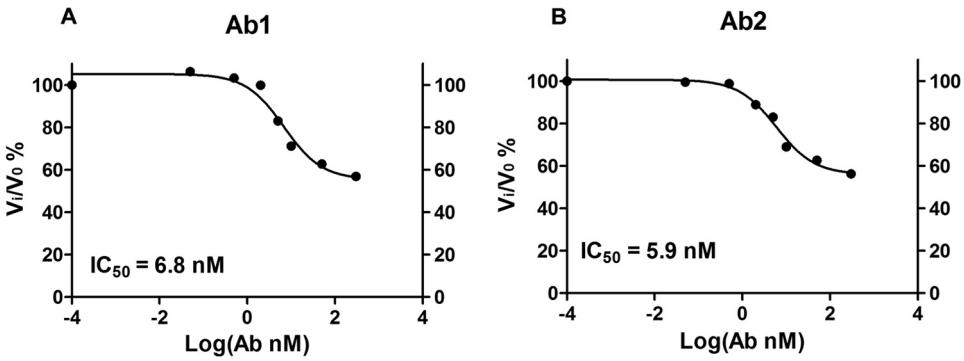

FIGURE 2. **Inhibitory antibodies decrease GLP-1 N-terminal clipping activity of plasma in *in vitro* reactions.** IC_{50} values of Ab1 and Ab2 for plasma DPP-IV activity against GLP-1 (FAM) (BACHEM 2000343) were 6.8 and 5.9 nM, respectively.

0.01 (90-min time point). In comparison, sitagliptin reduced plasma glucose level from 299.4 mg/dl to 242.1 mg/dl with $p < 0.01$ and from 287.6 mg/dl to 229.1 mg/dl with $p < 0.01$ at time points of 60 and 90 min, respectively. The increase in glucose tolerance is accompanied by a statistically significant or visible trend of increased plasma GLP-1 and insulin concentrations (Fig. 5, *B* and *C*).

When plasma GLP-1 concentrations of different groups were compared (Fig. 5*B*), we observed that administrating Ab1 raised plasma GLP-1 concentration, although at weaker efficacy in

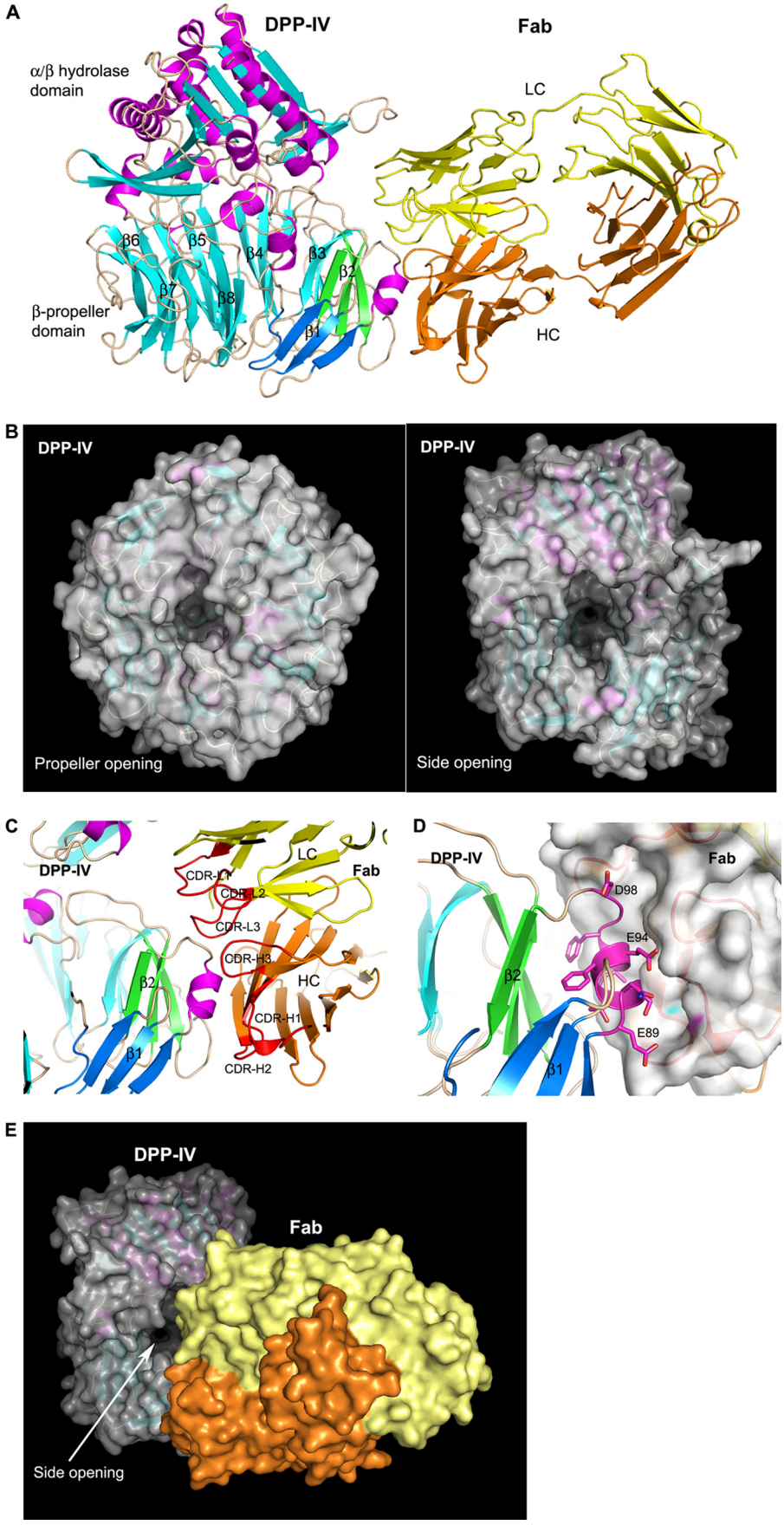
A
DPP-IV
Fab
α/β hydrolase domain
LC
β6
β5
β4
β3
β2
β7
β8
β-propeller domain
β1
HC
B
DPP-IV
Propeller opening
DPP-IV
Side opening
C
DPP-IV
LC
Fab
CDR-L1
CDR-L2
CDR-L3
CDR-H3
HC
β2
CDR-H1
β1
CDR-H2
D
DPP-IV
Fab
D98
E94
β2
E89
β1
E
DPP-IV
Fab
Side opening

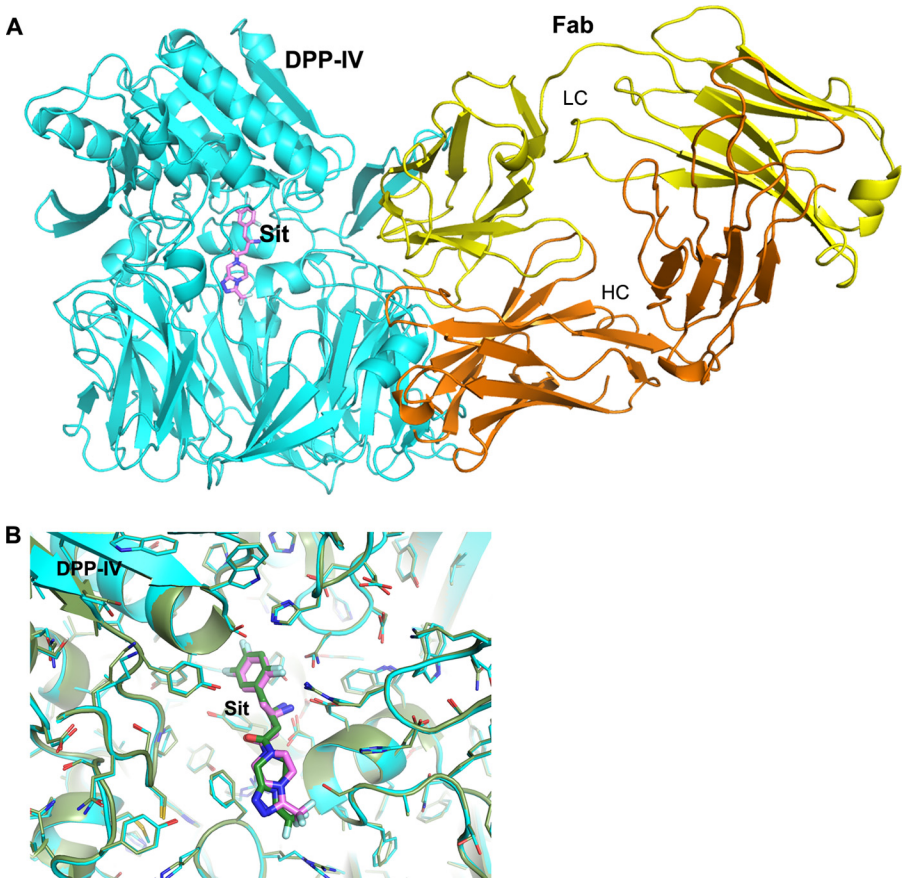

FIGURE 4. **Co-crystal structure of ternary complex of DPP-IV with Ab1 Fab and sitagliptin.** *A*, overall view of the ternary complex, with DPP-IV colored in *cyan*; sitagliptin (denoted as *Sit*; shown in stick representation) is colored *magenta* for carbon, *red* for oxygen, *blue* for nitrogen, and *pale cyan* for fluorine. Fab is shown in both ribbon and molecular surface representations as in Fig. 3. *LC*, light chain; *HC*, heavy chain. *B*, comparison of sitagliptin bindings at the active sites of rat DPP-IV·Ab1 Fab complex and human DPP-IV. The complex structure of human DPP-IV with sitagliptin (PDB code: 1X70) is colored in *dark green*.

comparison with sitagliptin under experimental conditions. The effects of sitagliptin in increasing GLP-1 concentration were found to be statistically significant for all of the time points assayed. For Ab1, the increase in plasma GLP-1 reached statistical significance at 10 min after glucose challenge.

Furthermore, we also compared plasma insulin concentrations of different treatment groups. In comparison with glucose and GLP-1 levels, the trend of plasma insulin concentration of the Ab1 group showed nearly identical increase as that of sitagliptin, although neither group reached statistical significance at any of the time points assayed (Fig. 5*C*). Taken together, the results from this experiment demonstrate that an inhibitory antibody for DPP-IV is capable of achieving *in vivo* efficacy to increase plasma GLP-1 concentration and improve glucose tolerance.

DISCUSSION

Small molecule inhibitors targeting DPP-IV enzymatic activity represent a new class of antihyperglycemic agents for treatment of type 2 diabetes (13, 20, 43). Until now, large molecule therapies targeting DPP-IV have not been reported. Antibody-based large molecule therapies offer long *in vivo* half-lives and high degrees of target specificity, which generally impart improved efficacy over small molecule drugs. Here we report the discovery of an inhibitory antibody against DPP-IV that binds the β-propeller domain of DPP-IV and partially inhibits its GLP-1 cleavage activity by impeding substrate access to the catalytic site. Importantly, this antibody demonstrated its efficacy in improving glucose tolerance and raising plasma GLP-1 concentrations in a diabetic animal model.

In this study, we identified only partial inhibitory antibodies against rat DPP-IV. DPP-IV activity is involved in many functions of the metabolic, endocrine, and immune systems and is implicated in regulating cell adhesion, cancer growth, and bone marrow mobilization (44). Its physiological substrates include GIP, GLP-1, substance P, and chemokines SDF1a (stromal cell-derived factor 1 a) and SDF1b (45). SDF1 chemokines are

FIGURE 3. **Crystal structure of DPP-IV in complex with the Fab of Ab1.** *A*, overall view of the complex structure. DPP-IV and Fab are shown in ribbon representation with DPP-IV colored in *magenta helices*, *cyan* β*-strands*, and *wheat loops* and Fab colored in *yellow* for light chain (*LC*) and *orange* for heavy chain (*HC*). The blades 1 and 2 in the β-propeller domain of DPP-IV are colored in *blue* and *green*, respectively. *B*, the propeller and side openings in DPP-IV. The protein is shown in both ribbon and molecular surface representations. *C* and *D*, Ab1 Fab recognition of DPP-IV. The CDR loops of Ab1 are colored in *red* and labeled as *CDR-L1*, *CDR-L2*, and *CDR-L3* and *CDR-H1*, *CDR-H2*, and *CDR-H3* for light chain and heavy chain, respectively. The Fab is shown in both ribbon and molecular surface representations in *D*. The key epitope residues of DPP-IV binding Fab are highlighted in stick representation. *E*, A1 Fab recognition of DPP-IV in molecular surface representation.

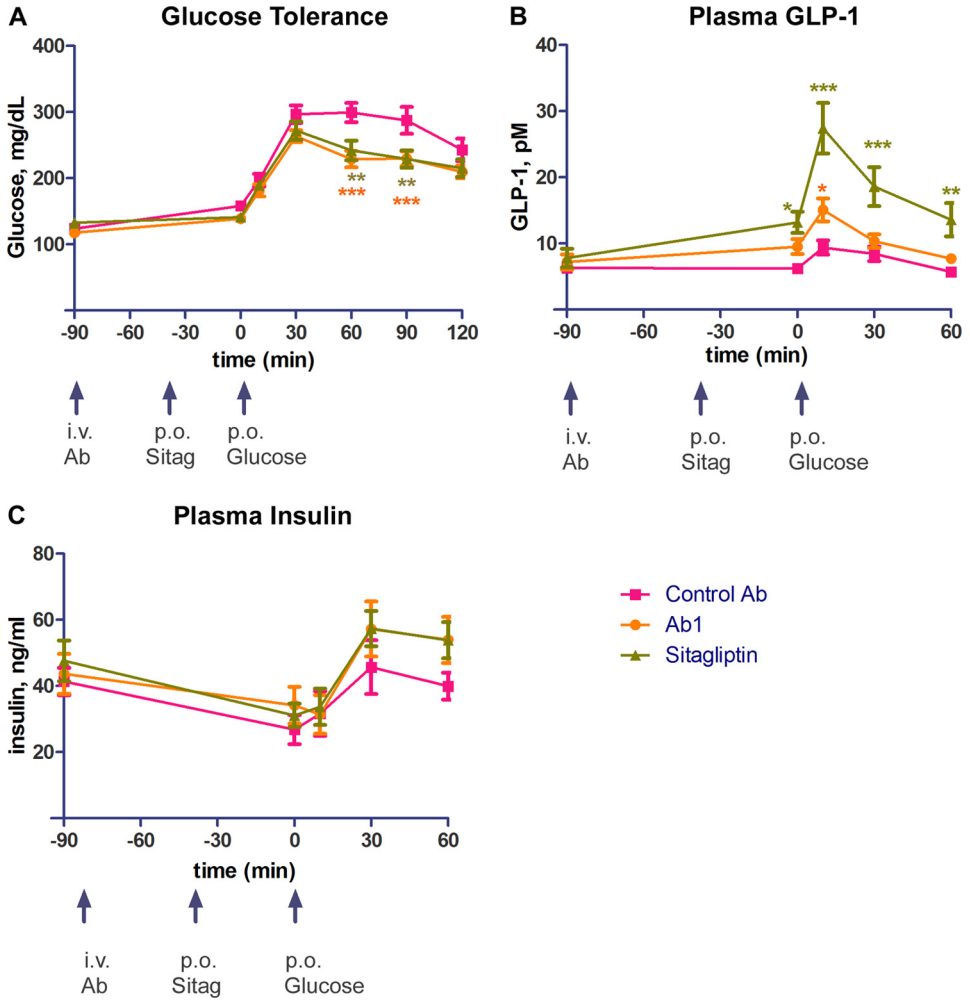

FIGURE 5. **Efficacy of Ab1 in Zucker fatty rat oral glucose tolerance test model.** *A–C*, plasma glucose concentrations (*A*), plasma GLP-1 concentrations (*B*), and plasma insulin concentrations (*C*) in rats administrated with Ab1, control mAb, or sitagliptin (denoted as *Sitag*). *i. v. Ab*, intravenous antibody administration; *p. o. Sitag*, sitagliptin by mouth; *p.o. Glucose*, glucose by mouth. *Error bars* indicate S.E. *, $p < 0.01$; **, $p < 0.001$; ***, $p < 0.0001$.

chemo-attractants for lymphocytes and monocytes, and regulate T- and B-lymphocyte development as well as mature lymphocyte survival. Substance P is a neurotransmitter/modulator and regulates nociception, pain transmission, smooth muscle contractions, and anxiety/stress-related responses. It is perceivable that long-term administration of an antibody with a partial inhibitory activity may have a better safety profile than a complete inhibitory antibody by permitting a low level of DPP-IV activity to degrade its physiological substrates. Future development of a fully inhibitory antibody against DPP-IV would enable us to compare efficacy and safety profiles between complete and partial inhibitory antibodies.

Our results demonstrate the potential of using a DPP-IV inhibitory antibody to improve glucose tolerance and plasma GLP-1 concentrations *in vivo*. However, whether an inhibitory DPP-IV antibody can become a successful incretin drug depends on factors beyond *in vivo* activity or pharmacokinetic and pharmacodynamic superiority over small molecule DPP-IV inhibitors. A detailed investigation of efficacy, drug safety, and dosing frequency is necessary to evaluate the clinical utility of inhibitory antibodies over small molecule DPP-IV inhibitors. The results observed in this study are the first step in exploring large molecule therapeutics to target DPP-IV activity and could potentially lead to an incretin agent that is long-lasting, specific, and efficacious in improving type 2 diabetic symptoms in humans.

Acknowledgment—The ALS is supported by the United States Department of Energy under Contract DE-AC03-76SF00098 at the Lawrence Berkeley National Laboratory.

REFERENCES

1. Mentlein, R. (1999) Dipeptidyl-peptidase IV (CD26)–role in the inactivation of regulatory peptides. *Regul. Pept.* **85,** 9–24
2. Rosenblum, J. S., and Kozarich, J. W. (2003) Prolyl peptidases: a serine protease subfamily with high potential for drug discovery. *Curr. Opin. Chem. Biol.* **7,** 496–504
3. Misumi, Y., Hayashi, Y., Arakawa, F., and Ikehara, Y. (1992) Molecular cloning and sequence analysis of human dipeptidyl peptidase IV, a serine proteinase on the cell surface. *Biochim. Biophys. Acta* **1131,** 333–336
4. Gorrell, M. D., Gysbers, V., and McCaughan, G. W. (2001) CD26: a multifunctional integral membrane and secreted protein of activated lymphocytes. *Scand. J. Immunol.* **54,** 249–264
5. Kameoka, J., Tanaka, T., Nojima, Y., Schlossman, S. F., and Morimoto, C. (1993) Direct association of adenosine deaminase with a T cell activation

antigen, CD26. *Science* **261,** 466–469
6. Marguet, D., Bernard, A. M., Vivier, I., Darmoul, D., Naquet, P., and Pierres, M. (1992) cDNA cloning for mouse thymocyte-activating molecule: a multifunctional ecto-dipeptidyl peptidase IV (CD26) included in a subgroup of serine proteases. *J. Biol. Chem.* **267,** 2200–2208
7. Rasmussen, H. B., Branner, S., Wiberg, F. C., and Wagtmann, N. (2003) Crystal structure of human dipeptidyl peptidase IV/CD26 in complex with a substrate analog. *Nat. Struct. Biol.* **10,** 19–25
8. Weihofen, W. A., Liu, J., Reutter, W., Saenger, W., and Fan, H. (2004) Crystal structure of CD26/dipeptidyl-peptidase IV in complex with adenosine deaminase reveals a highly amphiphilic interface. *J. Biol. Chem.* **279,** 43330–43335
9. Weihofen, W. A., Liu, J., Reutter, W., Saenger, W., and Fan, H. (2005) Crystal structures of HIV-1 Tat-derived nonapeptides Tat-(1–9) and Trp2-Tat-(1–9) bound to the active site of dipeptidyl-peptidase IV (CD26). *J. Biol. Chem.* **280,** 14911–14917
10. Aertgeerts, K., Ye, S., Tennant, M. G., Kraus, M. L., Rogers, J., Sang, B. C., Skene, R. J., Webb, D. R., and Prasad, G. S. (2004) Crystal structure of human dipeptidyl peptidase IV in complex with a decapeptide reveals details on substrate specificity and tetrahedral intermediate formation. *Protein Sci.* **13,** 412–421
11. Richter, B., Bandeira-Echtler, E., Bergerhoff, K., and Lerch, C. L. (2008) Dipeptidyl peptidase-4 (DPP-4) inhibitors for type 2 diabetes mellitus. *Cochrane Database Syst. Rev.* CD006739
12. Pederson, R. A., White, H. A., Schlenzig, D., Pauly, R. P., McIntosh, C. H., and Demuth, H. U. (1998) Improved glucose tolerance in Zucker fatty rats by oral administration of the dipeptidyl peptidase IV inhibitor isoleucine thiazolidide. *Diabetes* **47,** 1253–1258
13. Gallwitz, B. (2011) Small molecule dipeptidylpeptidase IV inhibitors under investigation for diabetes mellitus therapy. *Expert Opin. Investig. Drugs* **20,** 723–732
14. Vilsbøll, T., Krarup, T., Madsbad, S., and Holst, J. J. (2002) Defective amplification of the late phase insulin response to glucose by GIP in obese Type II diabetic patients. *Diabetologia* **45,** 1111–1119
15. Deacon, C. F. (2004) Therapeutic strategies based on glucagon-like peptide 1. *Diabetes* **53,** 2181–2189
16. Garber, A. J. (2010) Incretin-based therapies in the management of type 2 diabetes: rationale and reality in a managed care setting. *Am. J. Manag. Care* **16,** S187–0S194
17. Davidson, J. A. (2009) Advances in therapy for type 2 diabetes: GLP-1 receptor agonists and DPP-4 inhibitors. *Cleve. Clin. J. Med.* **76,** Suppl. 5, S28–S38
18. Balkan, B., Kwasnik, L., Miserendino, R., Holst, J. J., and Li, X. (1999) Inhibition of dipeptidyl peptidase IV with NVP-DPP728 increases plasma GLP-1 (7–36 amide) concentrations and improves oral glucose tolerance in obese Zucker rats. *Diabetologia* **42,** 1324–1331
19. Nauck, M. A., Kleine, N., Orskov, C., Holst, J. J., Willms, B., and Creutzfeldt, W. (1993) Normalization of fasting hyperglycaemia by exogenous glucagon-like peptide 1 (7–36 amide) in type 2 (non-insulin-dependent) diabetic patients. *Diabetologia* **36,** 741–744
20. Deacon, C. F. (2011) Dipeptidyl peptidase-4 inhibitors in the treatment of type 2 diabetes: a comparative review. *Diabetes Obes. Metab.* **13,** 7–18
21. Gupta, R., Walunj, S. S., Tokala, R. K., Parsa, K. V., Singh, S. K., and Pal, M. (2009) Emerging drug candidates of dipeptidyl peptidase IV (DPP IV) inhibitor class for the treatment of Type 2 Diabetes. *Curr. Drug Targets* **10,** 71–87
22. Engel, S. S., Williams-Herman, D. E., Golm, G. T., Clay, R. J., Machotka, S. V., Kaufman, K. D., and Goldstein, B. J. (2010) Sitagliptin: review of preclinical and clinical data regarding incidence of pancreatitis. *Int. J. Clin. Pract.* **64,** 984–990
23. Keating, G. M. (2010) Vildagliptin: a review of its use in type 2 diabetes mellitus. *Drugs* **70,** 2089–2112
24. Ligueros-Saylan, M., Foley, J. E., Schweizer, A., Couturier, A., and Kothny, W. (2010) An assessment of adverse effects of vildagliptin *versus* comparators on the liver, the pancreas, the immune system, the skin and in patients with impaired renal function from a large pooled database of Phase II and III clinical trials. *Diabetes Obes. Metab.* **12,** 495–509
25. Williams-Herman, D., Engel, S. S., Round, E., Johnson, J., Golm, G. T., Guo, H., Musser, B. J., Davies, M. J., Kaufman, K. D., and Goldstein, B. J. (2010) Safety and tolerability of sitagliptin in clinical studies: a pooled analysis of data from 10,246 patients with type 2 diabetes. *BMC Endocr. Disord.* **10,** 7
26. Lankas, G. R., Leiting, B., Roy, R. S., Eiermann, G. J., Beconi, M. G., Biftu, T., Chan, C. C., Edmondson, S., Feeney, W. P., He, H., Ippolito, D. E., Kim, D., Lyons, K. A., Ok, H. O., Patel, R. A., Petrov, A. N., Pryor, K. A., Qian, X., Reigle, L., Woods, A., Wu, J. K., Zaller, D., Zhang, X., Zhu, L., Weber, A. E., and Thornberry, N. A. (2005) Dipeptidyl peptidase IV inhibition for the treatment of type 2 diabetes: potential importance of selectivity over dipeptidyl peptidases 8 and 9. *Diabetes* **54,** 2988–2994
27. Nelson, A. L., Dhimolea, E., and Reichert, J. M. (2010) Development trends for human monoclonal antibody therapeutics. *Nat. Rev. Drug Discov.* **9,** 767–774
28. Carter, P. J. (2006) Potent antibody therapeutics by design. *Nat. Rev. Immunol.* **6,** 343–357
29. Wu, Y., Eigenbrot, C., Liang, W. C., Stawicki, S., Shia, S., Fan, B., Ganesan, R., Lipari, M. T., and Kirchhofer, D. (2007) Structural insight into distinct mechanisms of protease inhibition by antibodies. *Proc. Natl. Acad. Sci. U.S.A.* **104,** 19784–19789
30. Sun, J., Pons, J., and Craik, C. S. (2003) Potent and selective inhibition of membrane-type serine protease 1 by human single-chain antibodies. *Biochemistry* **42,** 892–900
31. Ganesan, R., Eigenbrot, C., Wu, Y., Liang, W. C., Shia, S., Lipari, M. T., and Kirchhofer, D. (2009) Unraveling the allosteric mechanism of serine protease inhibition by an antibody. *Structure* **17,** 1614–1624
32. Chan, J. C., Piper, D. E., Cao, Q., Liu, D., King, C., Wang, W., Tang, J., Liu, Q., Higbee, J., Xia, Z., Di, Y., Shetterly, S., Arimura, Z., Salomonis, H., Romanow, W. G., Thibault, S. T., Zhang, R., Cao, P., Yang, X. P., Yu, T., Lu, M., Retter, M. W., Kwon, G., Henne, K., Pan, O., Tsai, M. M., Fuchslocher, B., Yang, E., Zhou, L., Lee, K. J., Daris, M., Sheng, J., Wang, Y., Shen, W. D., Yeh, W. C., Emery, M., Walker, N. P., Shan, B., Schwarz, M., and Jackson, S. M. (2009) A proprotein convertase subtilisin/kexin type 9 neutralizing antibody reduces serum cholesterol in mice and nonhuman primates. *Proc. Natl. Acad. Sci. U.S.A.* **106,** 9820–9825
33. Leslie, A. (1992) *Joint CCP4+ESF-EAMCB Newsletter on Protein Crystallography*, Number 26, Collaborative Computational Project, Number 4, Daresbury Laboratory, Warrington, UK
34. Evans, P. (2006) Scaling and assessment of data quality. *Acta Crystallogr. D Biol. Crystallogr.* **62,** 72–82
35. Collaborative Computational Project, Number 4 (1994) The CCP4 suite: programs for protein crystallography. *Acta Crystallogr. D Biol. Crystallogr.* **50,** 760–763
36. Vagin, A., and Teplyakov, A. (2010) Molecular replacement with MOLREP. *Acta Crystallogr. D Biol. Crystallogr.* **66,** 22–25
37. Sheehan, S. M., Mest, H. J., Watson, B. M., Klimkowski, V. J., Timm, D. E., Cauvin, A., Parsons, S. H., Shi, Q., Canada, E. J., Wiley, M. R., Ruehter, G., Evers, B., Petersen, S., Blaszczak, L. C., Pulley, S. R., Margolis, B. J., Wishart, G. N., Renson, B., Hankotius, D., Mohr, M., Zechel, J. C., Michael Kalbfleisch, J., Dingess-Hammond, E. A., Boelke, A., and Weichert, A. G. (2007) Discovery of non-covalent dipeptidyl peptidase IV inhibitors which induce a conformational change in the active site. *Bioorg. Med. Chem. Lett.* **17,** 1765–1768
38. Che, Z., Olson, N. H., Leippe, D., Lee, W. M., Mosser, A. G., Rueckert, R. R., Baker, T. S., and Smith, T. J. (1998) Antibody-mediated neutralization of human rhinovirus 14 explored by means of cryoelectron microscopy and X-ray crystallography of virus-Fab complexes. *J. Virol.* **72,** 4610–4622
39. Emsley, P., and Cowtan, K. (2004) Coot: model-building tools for molecular graphics. *Acta Crystallogr. D Biol. Crystallogr.* **60,** 2126–2132
40. Murshudov, G. N., Vagin, A. A., and Dodson, E. J. (1997) Refinement of macromolecular structures by the maximum-likelihood method. *Acta Crystallogr. D Biol. Crystallogr.* **53,** 240–255
41. Longenecker, K. L., Stewart, K. D., Madar, D. J., Jakob, C. G., Fry, E. H., Wilk, S., Lin, C. W., Ballaron, S. J., Stashko, M. A., Lubben, T. H., Yong, H., Pireh, D., Pei, Z., Basha, F., Wiedeman, P. E., von Geldern, T. W., Trevillyan, J. M., and Stoll, V. S. (2006) Crystal structures of DPP-IV (CD26) from rat kidney exhibit flexible accommodation of peptidase-selective in-

hibitors. *Biochemistry* **45,** 7474–7482
42. Kim, D., Wang, L., Beconi, M., Eiermann, G. J., Fisher, M. H., He, H., Hickey, G. J., Kowalchick, J. E., Leiting, B., Lyons, K., Marsilio, F., McCann, M. E., Patel, R. A., Petrov, A., Scapin, G., Patel, S. B., Roy, R. S., Wu, J. K., Wyvratt, M. J., Zhang, B. B., Zhu, L., Thornberry, N. A., and Weber, A. E. (2005) (2*R*)-4-oxo-4-[3-(trifluoromethyl)-5,6-dihydro[1,2,4]triazolo[4,3-a]pyrazin-7(8*H*)-yl]-1-(2,4,5-trifluorophenyl)butan-2-amine: a potent, orally active dipeptidyl peptidase IV inhibitor for the treatment of type 2 diabetes. *J. Med. Chem.* **48,** 141–151
43. Chahal, H., and Chowdhury, T. A. (2007) Gliptins: a new class of oral hypoglycaemic agent. *QJM* **100,** 671–677
44. Gorrell, M. D. (2005) Dipeptidyl peptidase IV and related enzymes in cell biology and liver disorders. *Clin. Sci.* **108,** 277–292
45. Kirby, M., Yu, D. M., O'Connor, S., and Gorrell, M. D. (2010) Inhibitor selectivity in the clinical application of dipeptidyl peptidase-4 inhibition. *Clin. Sci.* **118,** 31–41
46. DeLano, W. L. (2010) *The PyMOL Molecular Graphics System*, version 1.3r1, Schrödinger, LLC, New York